


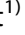




# Artificial neural network and energy budget method to predict daily evaporation of Boudaroua reservoir (northern Morocco)

Hicham En-nkhili<sup>1)</sup>✉ , Imane Nizar<sup>2)</sup> , Mohammed Igouzal<sup>1)</sup> ,  
Azzeddin Touazit<sup>1)</sup> , Nizar Youness<sup>1)</sup> , Issam Etebaai<sup>3)</sup> 

<sup>1)</sup> Ibn Tofail University, Faculty of Science, Department of Physics, Laboratory of Electronic Systems, Information Processing, Mechanics and Energy, University campus, B.P. 242, 14000 Kenitra, Morocco

<sup>2)</sup> University Hassan II, Higher Normal School of Technical Education (ENSET), Computer Science, Artificial Intelligence and Cybersecurity (IIACS), Mohammedia, Casablanca, Morocco

<sup>3)</sup> Abdelmalek Essaadi University, Faculty of Science and Technique, Department of Earth and Environmental Sciences, Team of Applied Geosciences and Geological Engineering, Al Hoceima, Morocco

RECEIVED 12.10.2022

ACCEPTED 13.02.2023

AVAILABLE ONLINE 18.04.2023

**Abstract:** Evaporation is one of the main essential components of the hydrologic cycle. The study of this parameter has significant consequences for knowing reservoir level forecasts and water resource management. This study aimed to test the three artificial neural networks (feed-forward, Elman and nonlinear autoregressive network with exogenous inputs (NARX) models) and multiple linear regression to predict the rate of evaporation in the Boudaroua reservoir using the calculated values obtained from the energy budget method. The various combinations of meteorological data, including solar radiation, air temperature, relative humidity, and wind speed, are used for the training and testing of the model's studies. The architecture that was finally chosen for three types of neural networks has the 4-10-1 structure, with contents of 4 neurons in the input layer, 10 neurons in the hidden layer and 1 neuron in the output layer. The calculated evaporation rate presents a typical annual cycle, with low values in winter and high values in summer. Moreover, air temperature and solar radiation were identified as meteorological variables that mostly influenced the rate of evaporation in this reservoir, with an annual average equal to  $4.67 \text{ mm}\cdot\text{d}^{-1}$ . The performance evaluation criteria, including the coefficient of determination ( $R^2$ ), root mean square error (RMSE) and mean absolute error (MAE) approved that all the networks studied were valid for the simulation of evaporation rate and gave better results than the multiple linear regression (MLR) models in the study area.

**Keywords:** artificial neural network, Boudaroua reservoir, energy budget, evaporation rate, meteorological data

## INTRODUCTION

Lakes, reservoirs and rivers are dynamic ecosystems that are constantly evolving and adapting to their environment (Igouzal and Maslouhi, 2005; El Qryefy *et al.*, 2021). Evaporation is a crucial climatic factor that impacts both plant and animal life. It is a non-linear process which occurs in nature due to temperature differences. Each year, millions of cubic meters of freshwater accumulate in reservoirs, lakes and dams from various sources such as rivers, precipitation and groundwater that evaporate and pass outside these ecosystems. For example, 61% of global

precipitation is lost through evaporation (Hunt *et al.*, 2020). Therefore, residual salts decrease water quality because the evaporation takes pure water only. Moreover, evaporation is the primary process of water transfer in the hydrologic cycle, which also significantly impacts how water balance is evaluated. Thus, the determination of reservoir evaporation is necessary for water and energy budget studies, reservoir level forecasts, water quality surveys, water management and the planning of hydraulic constructions (Malik, Kumar and Kisi, 2017). Furthermore, the physical parameters of the lakes and reservoirs, such as size, shape and depth, affect the pan evaporation (Antonopoulos, Giannou

and Antonopoulos, 2016). Evaporation is determined using direct methods by installing more precise and costly devices, including primarily pan evaporimeter and indirect methods, including empirical or semi-empirical models such as Penman–Monteith, Priestley–Taylor, De Bruin–Kejiman, Jensen–Haise, Makink, energy budget method, and mass transfer method (Hussein, 2017; Ansorge and Beran, 2019; Wang *et al.*, 2019) that rely on meteorological measurements such as solar radiation, air temperature, relative humidity and wind speed (Jhahharia *et al.*, 2009), while the applications of these techniques are often limited by data availability and completeness (Majidi *et al.*, 2015). Many researchers have significantly utilised artificial intelligence approaches to facilitate the estimation of evaporation rate and other weather variables like rainfall (Shafaei *et al.*, 2016) and relative humidity (El Azhari *et al.*, 2022). It is widely recognised that these techniques may represent the complex non-linearity of hydrologic processes and stochastic behaviour. For example, Al-Mukhtar (2021) compared four kinds of artificial intelligence methods: quantile regression forests, random forests, support vector machines and artificial neural networks with multiple linear regression models for modelling daily evaporation. They found that the quantile regression forests method is the most appropriate for predicting evaporation rates in arid to semi-arid climates such as Iraq.

Karami *et al.* (2021) investigated the neural network-based group method of data handling (GMDH-NN) to simulate the rate of evaporation in the synoptic station of the city of Garmsar located in Semnan province, Iran. They found that the sensitivity analysis results showed that the two input parameters of minimum temperature and percentage of relative humidity have a more significant effect on modelling evaporation rate than the other input parameters.

Patle, Chettri and Jhahharia (2020) used multiple linear regression (MLR) and artificial neural network (ANN) techniques to estimate monthly pan evaporation in two stations, Gangtok in Sikkim and Imphal in the Manipur states of India. Results showed a slightly better performance of the ANN models over the MLR models for predicting monthly pan evaporation in the study area.

Wang *et al.* (2017) compared six methods of artificial intelligence (AI): multi-layer perceptron (MLP), generalised

regression neural network (GRNN), fuzzy genetic (FG), least square support vector machine (LSSVM), multivariate adaptive regression spline (MARS), adaptive neuro-fuzzy inference systems with grid partition (ANFISGP) with two regression methods; multiple linear regression (MLR), and Stephens and Stewart model (SS) in predicting monthly pan evaporation across eight stations in different climatic zones in China. They approved that all AI models perform better than the regression methods, prioritising the MLP method.

Kisi (2015) investigated the accuracy of the least square support vector machine (LSSVM), multivariate adaptive regression splines (MARS) and M5 Model Tree (M5Tree) in modelling pan evaporation in three stations. The results showed that the LSSVM could estimate pan evaporation when local input and output data were available. However, if the data were unavailable, the MARS model would outperform the LSSVM model.

The studies have demonstrated the critical importance of different kinds of artificial intelligence in estimating the evaporation rate. Furthermore, it approved the superiority of the neural network approach over empirical equations using minimal weather parameters. The meteorological variables, including the mean air temperature ( $T_a$ ), solar radiation (SR), relative humidity (RH), and wind speed (WS), were used as inputs to predict the daily evaporation in the Boudaroua reservoir. In the first part, this study aims to calculate monthly and daily evaporation using the energy balance method and the one-dimensional FLake model. The second part examines the ability of three different artificial neural network methods: feed-forward, Elman, NARX models, and multiple linear regression (MLR) to estimate the rate of evaporation in the Boudaroua reservoir north of Morocco, with different combinations of climate inputs.

## MATERIALS AND METHODS

### STUDY AREA AND DATA USED

Boudaroua reservoir was built in 1936 and is located about 5 km from the town of Ouezzane in the north of Morocco, between latitudes 34°47' N and 05°27' W (Fig. 1). Until 1970, the waters of this reservoir were used as a source of drinking water. Nowadays,



**Fig. 1.** Satellite map of Boudaroua reservoir and their entourage; source: own elaboration based on Google maps

the pool is a tourist destination and a place of relaxation and entertainment. It has a surface area of about 13 ha and is 210 m in altitude. In addition, it has a mean depth of 5 m, and a maximum depth of 8 m. Direct precipitation and intermittent streams are the leading water suppliers of the reservoir (Etebaai, Damnati, and Taieb, 2010; En-nkhili *et al.*, 2020; En-nkhili *et al.*, 2021). During dry seasons, evaporation is the primary cause of water loss from the pool. However, during flooding, excess water is released downstream of the dam.

Surface water temperature is simulated by one dimensional FLake model which required input data: air temperature ( $T_a$ , °C), solar radiation ( $SR$ ,  $W \cdot m^{-2}$ ), vapour pressure (Pa) and wind speed ( $WS$ ,  $m \cdot s^{-1}$ ), in addition to physical parameters that characterise the lake such as mean depth and extinction coefficient, which is used to measure the absorption of light, albedo, and fetch. The meteorological data used were obtained by National Centers for Environmental Prediction/National Weather Service/NOAA/U.S. Department of Commerce (2015). Water temperature measurements in the Boudaroua reservoir during June 2019, October 2019, January 2020 and April 2021 (En-nkhili, Igouzal and Etebaai, 2022) were used to calibrate and validate the FLake model's parameters.

### ENERGY BUDGET METHOD

The Bowen ration energy budget (BREB) method is based on the conservation of energy law. It is considered one of the best methods for lake and reservoir evaporation calculation (Rosenberry *et al.*, 2007; Bozorgi *et al.*, 2020; Hojjati *et al.*, 2021). The expression of the energy budget for water surface body is given by Sturrock, Winter, and Rosenberry (1992), and Winter *et al.* (2003):

$$Q_c = Q_s - Q_{sr} + Q_L - Q_{Lr} - Q_b - H - LE + Q_{sed} + Q_v \quad (1)$$

where:  $Q_c$  = change in heat stored in the water body,  $Q_s$  = incoming solar shortwave radiation,  $Q_L$  = incident atmospheric longwave radiation,  $Q_{Lr}$  = reflected atmospheric longwave radiation,  $Q_b$  = back long-wave radiation emitted from the body of water surface,  $H$  = energy conducted from the water as sensible heat,  $LE$  = energy used for evaporation,  $Q_{sed}$  = heat transfer from water to the bottom sediments,  $Q_v$  = net energy from precipitation, inflow, and outflow,  $Q_{sr}$  = reflected solar shortwave radiation, (all parameters are expressed in  $W \cdot m^{-2}$ ), which is given by:

$$Q_{sr} = \alpha Q_s \quad (2)$$

where:  $\alpha$  = reflectivity of shortwave radiation of water, in general,  $\alpha$  is taken as 0.07 (Gianniu and Antnopoulos, 2007).

Incident atmospheric longwave radiation ( $Q_L$ ,  $W \cdot m^{-2}$ ), which is estimated by following equation:

$$Q_L = \varepsilon_a \sigma (T_a + 273.15)^4 \quad (3)$$

where:  $\sigma$  = Stefan-Boltzmann constant ( $5.67 \cdot 10^{-8} W \cdot m^{-2} \cdot K^{-4}$ ),  $\varepsilon_a$  = atmospheric emissivity,  $T_a$  = air temperature,  $Q_{Lr}$  is given by:

$$Q_{Lr} = \beta Q_L \quad (4)$$

$\beta$  = reflectivity of long-wave radiation of water, in general,  $\beta$  is taken as 0.03 (Gianniu and Antnopoulos, 2007).

The value  $Q_b$  ( $W \cdot m^{-2}$ ) is approached by the following equation:

$$Q_b = \varepsilon_w \sigma (T_e + 273.15)^4 \quad (5)$$

where:  $\varepsilon_w$  = water emissivity fixed at 0.97 (Bowie *et al.*, 1985),  $T_e$  = surface water temperature.

The basic equations used to calculate  $LE$  and  $H$  are:

$$LE = \rho_w L_v E \quad (6)$$

$$H = RLE \quad (7)$$

where:  $\rho_w$  = water density ( $1000 \text{ kg} \cdot \text{m}^{-3}$ ),  $R$  = Bowen ratio coefficient dimensionless,  $E$  = water evaporation,  $L_v$  = latent heat of evaporation ( $\text{J} \cdot \text{kg}^{-1}$ ), such as

$$L_v = 2.5 - 0.0024T \quad (8)$$

where,  $L_v$  expressed in  $\text{kJ} \cdot \text{g}^{-1}$  and  $T$  in °C

Finally, by combining the above equations, water evaporation is given by the following relation:

$$E = \frac{Q_s - Q_{sr} + Q_L - Q_{Lr} - Q_b - Q_c + Q_{sed} + Q_v}{(1 + R)\rho_w L_v} \quad (9)$$

The terms of  $Q_v$ ,  $Q_{sed}$  and  $Q_c$  are relatively small and are commonly neglected (Rosenberry *et al.*, 2007), so the expression becomes:

$$E = \frac{Q_s - Q_{sr} + Q_L - Q_{Lr} - Q_b}{(1 + R)\rho_w L_v} \quad (10)$$

### ARTIFICIAL NEURAL NETWORK

The three layers that make up an artificial neural network are the input layers, the hidden layer and the output layer. These layers are connected to artificial neurons by the weight  $w_{ij}$ .

The weighted input variables are added together to start information processing as follows:

$$I_j = \sum_{i=1}^n w_{ij} x_i + b_j \quad (11)$$

where:  $I_j$  = weighted input,  $i$  = layer index,  $j$  = neuron index,  $w_{ij}$  = assigned weight between the  $i_{th}$  layer and  $j_{th}$  neuron,  $x_i$  = value of the input that is stored in the  $i_{th}$  layer,  $b_j$  = bias with node  $j$ .

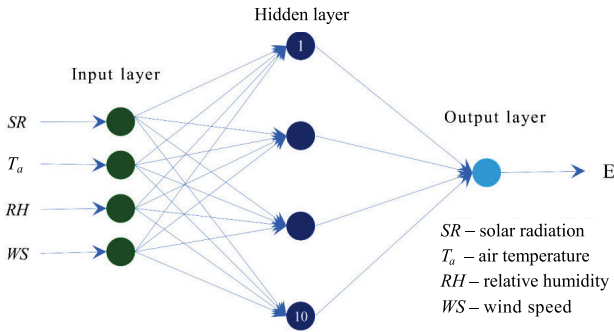
An activation function  $\varphi$ , determines the output of the  $j_{th}$  neuron such that:

$$y_j = \varphi(I_j) \quad (12)$$

Several activation functions can be used in ANNs, such as logistic (sigmoid), hyperbolic tangent (tanh) and Rectified Linear Unit Activation (ReLU). In the present study we selected the classical sigmoid function as the activation function.

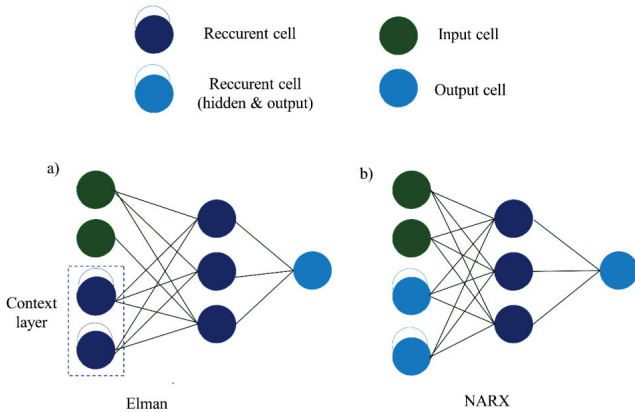
$$\varphi(I_j) = \frac{1}{1 + \exp(-I_j)} \quad (13)$$

The first neural network type used in this work is the feed-forward neural network that can be constructed in the layers so that information is processed from one layer to the next (Fig. 2).



**Fig. 2.** Architecture of the feed-forward neural network model used in this study using four input parameters; source: own study

The second and third types of ANN models are Elman and NARX neural networks, known as recurrent neural networks. Elman neural network (Elman, 1990) is a traditional neural network with an additional hidden layer input named the context layer (Fig. 3a). It is defined as partially recurrent and has a loop-back connection. The NARX neural network is like a multi-layered perceptron, except that it relies on the input and output regressors of the system to form the network from which it signals new input from the output (Fig. 3b).



**Fig. 3.** Recurrent model architectures: a) Elman, b) NARX; source: own study

Four different cases were examined depending on the number of input variables to assess the degree of effectiveness of the pan evaporation (Tab. 1).

**Table 1.** The different input combinations of meteorological parameters

Model	SR	T <sub>a</sub>	WS	RH
1	X			
2	X	X		
3	X	X	X	
4	X	X	X	X

Explanations: T<sub>a</sub> = air temperature, SR = solar radiation, RH = relative humidity, WS = wind speed, X = inclusion of the variable in the model. Source: own study.

To avoid convergence problems and minimal weighting factors, when extensive input and output values are used, it is prudent to standardise all external input and output values before passing them through the ANN network (Tayfur and Singh, 2005). Thus, the normalisation procedure assures better model performance. The following equation was used in this study to standardise the input and output data so that all values fell between 0 and 1.

$$x_i = \frac{X_i - X_{\min}}{X_{\max} - X_{\min}} \quad (14)$$

where: x<sub>i</sub> = standardised value, X<sub>i</sub> = original value, X<sub>max</sub>, X<sub>min</sub> = maximum and minimum variables, respectively.

Finally, the simulation outputs are denormalised to enable comparisons with the calculated evaporation data. Moreover, Levenberg-Marquardt (LM) training methods were used in this study to reduce mistakes between the target and output results. It uses the following equation for weight updating.

$$W_{i+1} = W_i + (J^T J + \theta I)^{-1} J^T e \quad (15)$$

where: W<sub>i</sub> = weight vector, J = Jacobian matrix, J<sup>T</sup> = transpose matrix of J, θ = learning parameter, I = identity matrix, e = error vector of the network.

### MULTIPLE LINEAR REGRESSION

Multiple linear regression (MLR) is a multivariate statistical technique used to model the nonlinear relationship between a dependent variable and one or more independent variables (Patle, Chettri and Jhajharia, 2020). It is used to estimate the pan evaporation for the study area.

The regression equation of y can be written as:

$$y = \alpha_0 + \alpha_1 x_1 + \alpha_2 x_2 + \dots + \alpha_k x_n \quad (16)$$

where: y = response variable, x<sub>1</sub>, x<sub>2</sub> ... x<sub>n</sub> = independent variables, α<sub>0</sub>, α<sub>1</sub>, α<sub>2</sub> ... α<sub>k</sub> = regression coefficients.

Moreover, the input variable combinations of the MLR models consist of the same meteorological variables used for the ANN models.

### PERFORMANCE EVALUATION CRITERIA

We use statistical equations, such as the coefficient of determination (R<sup>2</sup>), root mean square error (RMSE) and mean absolute error (MAE) to evaluate the performances of the models in this study.

$$R^2 = \frac{\sum_{i=1}^n (C_i - \bar{C}_i)(P_i - \bar{P}_i)}{\sqrt{(\sum_{i=1}^n (C_i - \bar{C}_i)^2)(\sum_{i=1}^n (P_i - \bar{P}_i)^2)}} \quad (17)$$

where: C<sub>i</sub> = values calculated by the energy budget method, P<sub>i</sub> = predicted values, C̄<sub>i</sub> and P̄<sub>i</sub> = mean calculated and predicted values, respectively, n = total number of data.

$$RMSE = \sqrt{\frac{\sum_{i=1}^n (C_i - P_i)^2}{n}} \quad (18)$$



$$MAE = \frac{1}{n} \sum_{i=1}^n |C_i - P_i| \quad (19)$$

## RESULTS AND DISCUSSION

### SURFACE WATER AND AIR TEMPERATURE

The mean monthly variation of air temperature ( $T_a$ ) and water surface temperature ( $T_w$ ) of the period 2019–2020 are presented in Figure 4. The average annual air and reservoir surface temperatures are 17.81 and 15.85°C, respectively. The water temperatures during all months are lower than air temperatures except for November. However, the water surface reservoir temperature was almost equal to the air temperature for two months: December and January. Therefore, the lake wins energy in spring and summer ( $T_w < T_a$ ), provides energy in November ( $T_w > T_a$ ) and thermal equilibrium with the atmosphere in December and January ( $T_w = T_a$ ). The result of this study is similar to other studies, such as Hojjati *et al.* (2021), who estimated evaporation in the Alavian reservoir (Iran), and Majidi *et al.* (2015) in the Doosti reservoir, where they found that the monthly air temperature during summer is higher than water surface temperature.

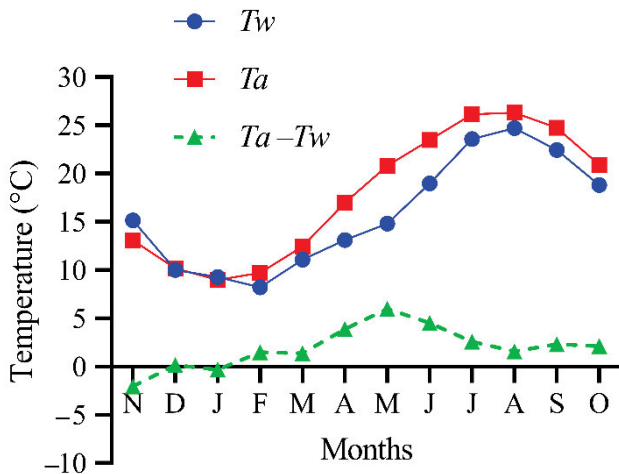


Fig. 4. The mean monthly variation of air temperature ( $T_a$ ) and water surface temperature ( $T_w$ ) of Boudaroua reservoir; source: own study

### ENERGY BUDGET METHOD

The mean monthly energy component values for the Boudaroua reservoir during 2019–2020 are presented in Figure 5. The first component of the energy budget is net shortwave radiation ( $Q_{ns} = Q_s - Q_{sr}$ ), which characterises the energy source of the physical and biological activities of the ecosystem. Net shortwave radiation ( $Q_{ns}$ ) has an average annual value of 225.94  $W \cdot m^{-2}$ . Moreover, the mean annual values of incoming ( $Q_L - Q_{Lr}$ ) and outgoing ( $Q_b$ ) longwave radiation are 307.34 and 394.3  $W \cdot m^{-2}$ , respectively, and indicate an annual mean energy loss of 86.96  $W \cdot m^{-2}$ .

Sensitive heat ( $H$ ) is due to conduction and convection, whereas latent heat ( $LE$ ) is the heat transported by water that evaporates. The values of  $H$  and  $LE$  are negative in the case of the Boudaroua reservoir. Also, heat being evacuated from surface

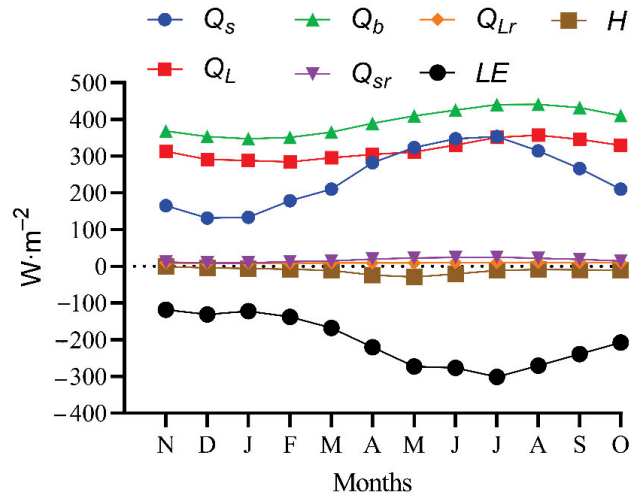


Fig. 5. The mean monthly variation of the energy budget components for Boudaroua reservoir during 2019–2020;  $Q_s$  = incoming solar shortwave radiation,  $Q_b$  = back long-wave radiation emitted from the body of water surface,  $Q_{Lr}$  = reflected atmospheric longwave radiation,  $H$  = sensitive heat,  $Q_L$  = incident atmospheric longwave radiation,  $Q_{sr}$  = reflected solar shortwave radiation,  $LE$  = latent heat; source: own study

water with latent heat is more critical than sensitive heat. In general, the mean evaporation rate of 4.67  $mm \cdot d^{-1}$  for the estimation period is equivalent to a mean annual loss with sensitive heat energy of 12  $mm \cdot d^{-1}$  and a mean yearly latent heat loss of 205.54  $mm \cdot d^{-1}$ . In addition, Figure 6 shows the daily and monthly average evaporation values generated by the energy balance method in the Boudaroua reservoir over one year (November 2019–October 2020) using Equation (10). According

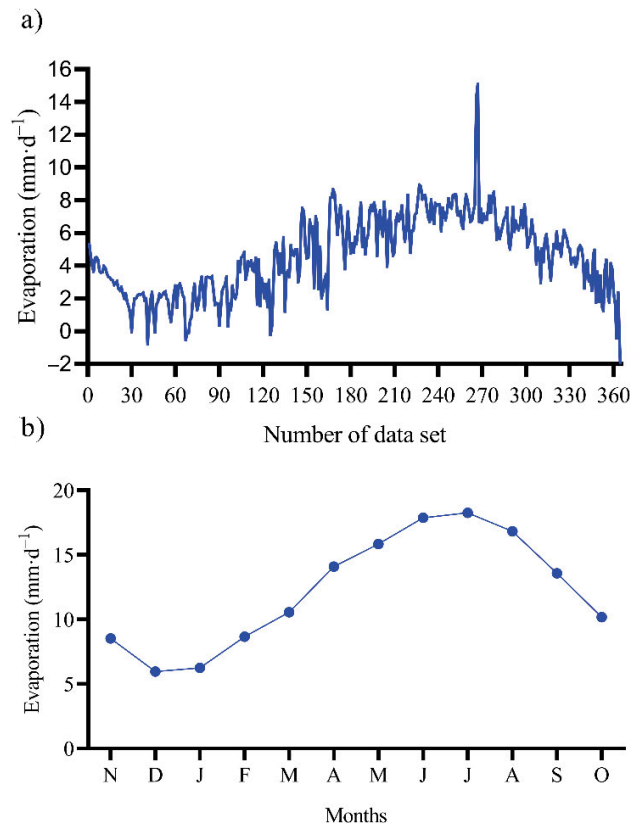


Fig. 6. Calculated evaporation values of Boudaroua reservoir during 2019–2020: a) daily, b) monthly; source: own study

to this figure, the daily and the monthly evaporation decreases in early fall and takes the minimum value in winter (the minimum value is  $0.03 \text{ mm}\cdot\text{d}^{-1}$ , and the minimum mean monthly value is  $1.76 \text{ mm}\cdot\text{d}^{-1}$ ) and begins to increase in the spring reaching its highest values in July (the maximum is  $15.10 \text{ mm}\cdot\text{d}^{-1}$ , the maximum mean monthly value is  $7.84 \text{ mm}\cdot\text{d}^{-1}$ ). However, the evaporation rate starts to decrease at the end of August due to a decrease in air temperature. Moreover, the mean annual evaporation rate from the Boudaroua reservoir is  $4.67 \text{ mm}\cdot\text{d}^{-1}$ . This value is considerable, especially since the pool is fed only by runoff in the rainy season. Consequently, the reservoir level decreases over time, harming the ecosystem's living beings. Additionally, the negative values of evaporation rates (Fig. 6a), which means condensation of water recorded in some data, are relative to the rapid variation in air temperature and vapour pressure.

### ESTIMATION OF DAILY PAN EVAPORATION

In this work, we applied the feed-forward, Elman, NARX neural network models and the multiple linear regression (MLR) model to estimate the rate of evaporation in the Mediterranean reservoir. Four meteorological variables (solar radiation (SR), air temperature ( $T_a$ ), relative humidity (RH) and wind speed (WS)) were used as inputs variables, and the evaporation values calculated by the energy budget components were used as the output variables in the generation of three artificial neural network (ANN) models. Before training and validation, the input and output variables were standardised using Equation (14). The 364 input data were divided into a training set of 273 (75%) and validation of 91 (25%) to generate the ANN models. Moreover, after training many times to determine the best ANN model architecture, the number of neurons in the hidden layer selected for the performance model is 10. The simulations showed that an increase or decrease in the hidden layer and the number of neurons in the hidden layer have no significant improvement to the evaporation predicted. Therefore, the most appropriate model of the structure is 4-10-1, which means that the model consists of 4 input variables, 10 neurons in the hidden layer and 1 neuron in the output layer.

The statistical performance evaluation criteria were *RMSE*, mean absolute error (*MAE*) and coefficient of determination ( $R^2$ ) of the four models for the Boudaroua reservoir and are presented in Table 2. The results show that increasing the number of input variables combinations to the regression models improves the accuracy of pan evaporation predictions. Model 4 for feed-forward, Elman and NARX neural network models has the smallest *RMSE* ( $0.0265$ ,  $0.0273$  and  $0.0266 \text{ mm}\cdot\text{d}^{-1}$  for training;  $0.0186$ ,  $0.0187$  and  $0.0196 \text{ mm}\cdot\text{d}^{-1}$  for validation), the smallest *MAE* ( $0.0189$ ,  $0.0186$  and  $0.0189 \text{ mm}\cdot\text{d}^{-1}$  for training;  $0.0133$ ,  $0.0135$  and  $0.0137 \text{ mm}\cdot\text{d}^{-1}$  for validation) and the highest  $R^2$  ( $0.9689$ ,  $0.9676$  and  $0.9691$  for training;  $0.9863$ ,  $0.9857$  and  $0.9846$  for validation), respectively. The same performances of the ANN are found by Al-Mukhtar (2021). Similarly, MLR model 4 has the smallest *RMSE* ( $0.5198$  and  $0.5133 \text{ mm}\cdot\text{d}^{-1}$ ), *MAE* ( $0.4070$  and  $0.3684 \text{ mm}\cdot\text{d}^{-1}$ ), and the highest  $R^2$  ( $0.9444$  and  $0.9816$ ) (Tab. 3). Therefore, the combined influence of all meteorological parameters on the evaporation rate should be considered. Additionally, the results showed that ANN and MLR predictive models could be used for accurate predictions because they have a high determination coefficient  $R^2$ . While comparing the *RMSE* and *MAE* of both models, ANN models showed superior predictive performance compared to the MLR models. They had a sufficient accuracy level in predicting the rate of evaporation. Many researchers also reported that evaporation estimation done through the ANN model was better than an estimate through the MLR model (Ali and Saraf, 2015; Malik, Kumar and Rai, 2018). Thus, all the ANN models do not have significant differences for the three criteria, showing the influence of solar radiation and air temperature on pan evaporation. This conclusion is confirmed by the results obtained in Table 4, which shows the strong correlation between solar radiation and pan evaporation. There is a high correlation between air temperature and pan evaporation as well. It was also observed that the relative humidity has a significant negative correlation, which is responsible for decreasing the pan evaporation. Wind speed has a very weak negative correlation with pan evaporation; thus, it has no crucial role in evaporation. This is due to the geographical location of the reservoir kept from the east and west winds and the presence of trees that act as obstacles to the wind and therefore decrease its speed.

**Table 2.** Comparison of feed-forward, Elman and NARX neural network models for Boudaroua reservoir

Model	Training									Validation								
	model																	
	feed-forward			Elman			NARX			feed-forward			Elman			NARX		
	<i>RMSE</i>	<i>MAE</i>	$R^2$	<i>RMSE</i>	<i>MAE</i>	$R^2$	<i>RMSE</i>	<i>MAE</i>	$R^2$	<i>RMSE</i>	<i>MAE</i>	$R^2$	<i>RMSE</i>	<i>MAE</i>	$R^2$	<i>RMSE</i>	<i>MAE</i>	$R^2$
1	0.0325	0.0255	0.9533	0.0334	0.0267	0.9519	0.0336	0.0268	0.9508	0.0288	0.0222	0.9701	0.0285	0.0226	0.9724	0.0286	0.0225	0.9508
2	0.0286	0.0216	0.9643	0.0385	0.0304	0.9341	0.0286	0.0211	0.9637	0.0221	0.0146	0.9802	0.0331	0.0211	0.9759	0.0226	0.0154	0.9793
3	0.0265	0.0195	0.9687	0.0294	0.0216	0.9617	0.0288	0.0212	0.99632	0.0215	0.0143	0.9813	0.0218	0.0156	0.9834	0.0224	0.0151	0.9806
4	<b>0.0265</b>	<b>0.0189</b>	<b>0.9689</b>	<b>0.0273</b>	<b>0.0186</b>	<b>0.9676</b>	<b>0.0266</b>	<b>0.0189</b>	<b>0.9691</b>	<b>0.0186</b>	<b>0.0133</b>	<b>0.9863</b>	<b>0.0187</b>	<b>0.0135</b>	<b>0.9857</b>	<b>0.0196</b>	<b>0.0137</b>	<b>0.9846</b>

Explanations: *RMSE* = root mean square error, *MAE* = mean absolute error,  $R^2$  = coefficient of determination, values bolded = distinguish the model characterised by low values of *RMSE* and *MAE* and high values of  $R^2$  compared to other models.

Source: own study.

**Table 3.** Statistical performance evaluation criteria for multiple linear regression (MLR)

Model	MLR					
	training			validation		
	RMSE	MAE	R <sup>2</sup>	RMSE	MAE	R <sup>2</sup>
1	0.5674	0.4559	0.9456	0.5408	0.3898	0.9800
2	0.5355	0.4255	0.9514	0.5351	0.3873	0.9808
3	0.5208	0.4084	0.9542	0.5435	0.3922	0.9806
4	<b>0.5198</b>	<b>0.4070</b>	<b>0.9544</b>	<b>0.5133</b>	<b>0.3684</b>	<b>0.9816</b>

Explanations: RMSE, MAE, R<sup>2</sup>, and values bolded as in Tab. 2. Source: own study.

Figure 7 shows a comparison of evaporation values modelled by models with evaporation calculated by the energy budget (EB) method for testing data of structure 4-10-1: a) feed-forward, b) Elman, c) NARX, d) MLR. It can be observed that there is a good correlation between the energy budget method pan evaporation and each of the other models, which is also consistent with the high values of the determination coefficient R<sup>2</sup> ranging from 0.9816 to 0.9863.

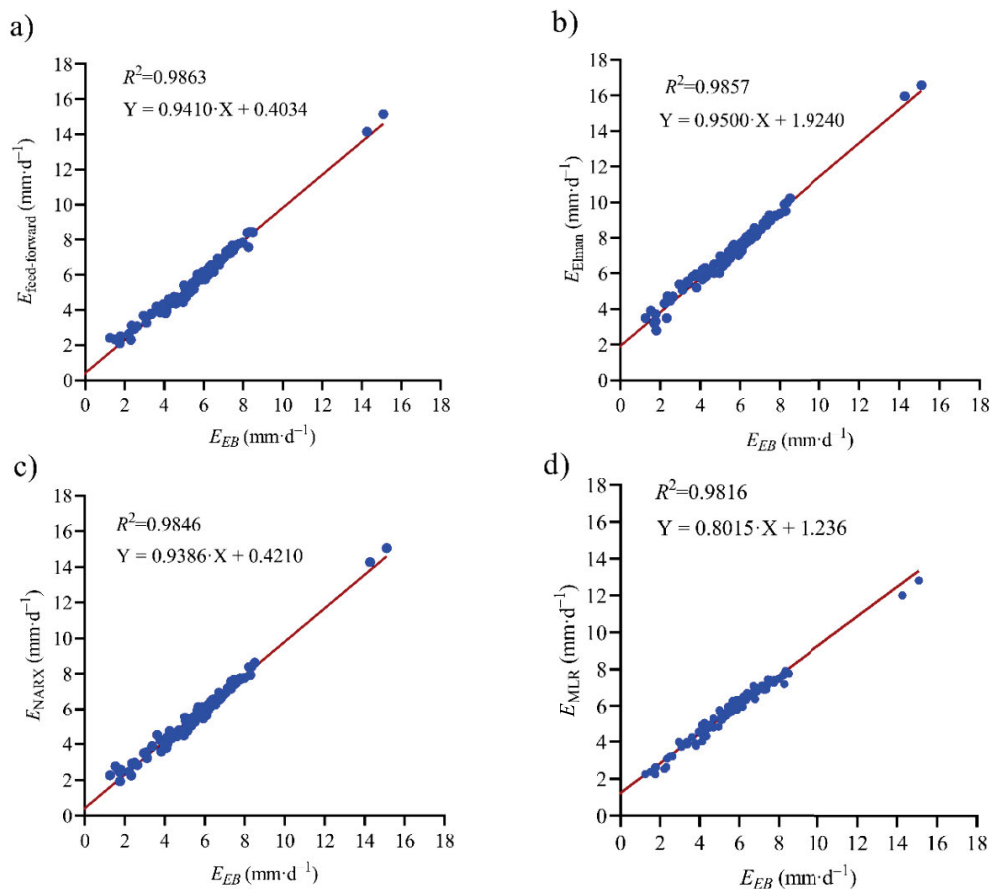
In addition, Figure 8 shows the calculated and modelled evaporation rate over time: Figure 8a represents model 4 with an average annual evaporation rate for feed-forward of 4.63 mm·d<sup>-1</sup>, for Elman, it is 4.17 mm·d<sup>-1</sup>, and for NARX – 4.61 mm·d<sup>-1</sup>. While Figure 8b represents model 3, the mean yearly evaporation rate

**Table 4.** Correlation between dependent and independent variables for Boudaroua reservoir

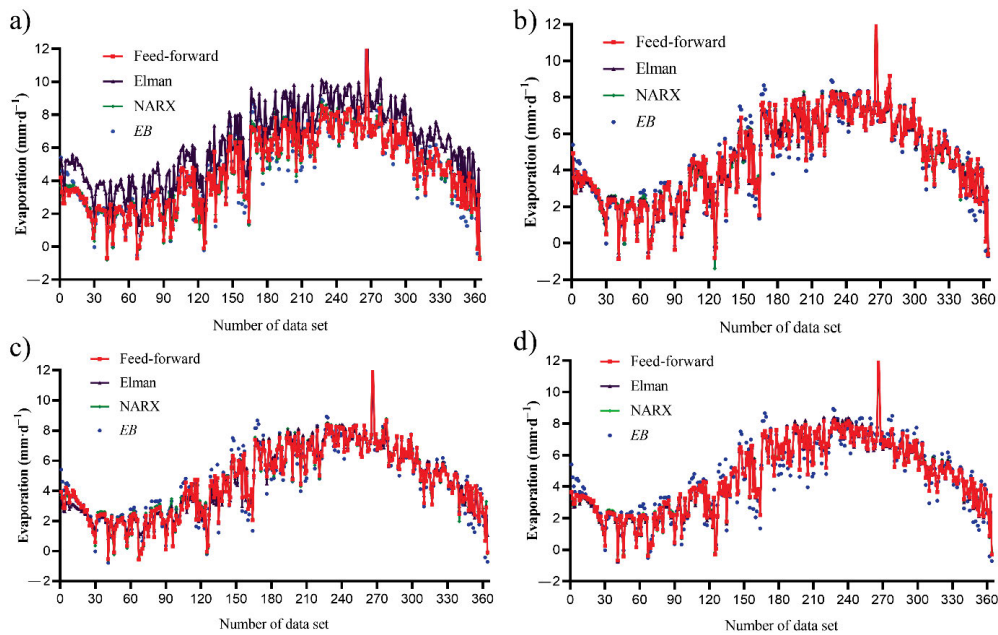
Variable	T <sub>a</sub>	SR	WS	RH	E
T <sub>a</sub>	1				
SR	0.67	1			
WS	-0.28	-0.21	1		
RH	-0.80	-0.46	0.30	1	
E	0.70	0.97	-0.25	-0.50	1

Explanations: T<sub>a</sub> = air temperature, SR = solar radiation, WS = wind speed, RH = relative humidity, E = water evaporation. Source: own study.

for feed-forward and Elman is equal to 4.62 mm·d<sup>-1</sup>, and for the NARX neural network, it is 4.64 mm·d<sup>-1</sup>. Moreover, Figure 8c presents the calculated and modelled evaporation over time for model 2, the mean yearly evaporation rate for feed-forward is 4.61 mm·d<sup>-1</sup>, for Elman, it is 4.63 mm·d<sup>-1</sup>, and for the NARX model, it is 4.64 mm·d<sup>-1</sup>. Finally, Figure 8d represents model 1, the mean yearly evaporation rate for feed-forward is 4.63 mm·d<sup>-1</sup>, and for Elman and NARX models – 4.62 mm·d<sup>-1</sup>. These results show that all ANN models studied were valid for predicting evaporation at the Boudaroua reservoir, with an advantage for the feed-forward model compared with the mean yearly value obtained by the energy budget method, which equals 4.67 mm·d<sup>-1</sup>.



**Fig. 7.** Modelled versus calculated daily evaporation (E) by such models for testing data: a) feed-forward, b) Elman, c) NARX, d) MLR; EB = energy budget; source: own study



**Fig. 8.** Boudaroua reservoir evaporation prediction by: a) four input variables:  $SR$ ,  $T_a$ ,  $RH$  and  $WS$ , b) three input variables:  $SR$ ,  $T_a$  and  $WS$ , c) two input variables:  $SR$  and  $T_a$ , d) one input variable:  $SR$ ;  $EB$  = energy budget,  $T_a$ ,  $SR$ ,  $WS$ ,  $RH$ ,  $EB$  as in Tab. 4; source: own study

## CONCLUSIONS

In this study, the daily values of evaporation in the Boudaroua reservoir were simulated from November 2019 to October 2020 using the energy balance method and the FLake model. This latter simulates the daily variations of reservoir water temperature with depth, the surface temperature, the change in the thermal content of the lake and the energy budget component. Therefore, the daily evaporation values were calculated using the energy budget method, considered a reference method. The three artificial neural network models (feed-forward, Elman, and NARX network) and MLR models are used to predict the evaporation rate by different meteorological data inputs. The data was divided into 273 data sets for training and 91 for validation. Model 4, with inputs of solar radiation, air temperature, relative humidity, and wind speed, provides the best evaporation estimations among the input combinations tried in this work. Based on the correlation coefficient, it was found that solar radiation and air temperature substantially impact the evaporation processes. The model's performances were assessed using three different statistical criteria  $RMSE$ ,  $MAE$ , and  $R^2$ . The four models were satisfactory in predicting the daily evaporation of the reservoir. However, the comparative performance of the ANN and MLR approaches showed that the former was more suitable for estimating daily evaporation in the study area.

## REFERENCES

Ali, J. and Saraf, S. (2015) "Evaporation modelling by using artificial neural network and multiple linear regression technique," *International Journal of Agricultural and Food Science*, 5, pp. 125–133.

Al-Mukhtar, M. (2021) "Modeling the monthly pan evaporation rates using artificial intelligence methods: A case study in Iraq,"

*Environmental Earth Sciences*, 80(1). Available at: <https://doi.org/10.1007/s12665-020-09337-0>.

Ansonge, L. and Beran, A. (2019) "Performance of simple temperature-based evaporation methods compared with a time series of pan evaporation measures from a standard 20 m<sup>2</sup> tank," *Journal of Water and Land Development*, 41, pp. 1–11. Available at: <https://doi.org/10.2478/jwld-2019-0021>.

Antonopoulos, V.Z., Gianniu, S.K. and Antonopoulos, A.V. (2016) "Artificial neural networks and empirical equations to estimate daily evaporation: application to Lake Vegoritis, Greece," *Hydrological Sciences Journal*, 61(14), pp. 2590–2599. Available at: <https://doi.org/10.1080/02626667.2016.1142667>.

Bowie, G.L. et al. (1985) *Rates, constants, and kinetics formulations in surface water quality modeling*. 2nd edn. Athens, Georgia: U.S. Environmental Protection Agency.

Bozorgi, A. et al. (2020) "Comparison of methods to calculate evaporation from reservoirs," *International Journal of River Basin Management*, 18(1), pp. 1–12. Available at: <https://doi.org/10.1080/15715124.2018.1546729>.

El Azhari, K. et al. (2022) "Development of a neural statistical model for the prediction of relative humidity levels in the region of Rabat-Kenitra, North West Morocco," *Journal of Water and Land Development*, 54, pp. 13–20. Available at: <https://doi.org/10.24425/jwld.2022.141550>.

El Qryefy, M. et al. (2021) "Hydrochemical characteristics and water quality assessment of Lake Dayet Erroumi – Khemisset, Morocco," *Journal of Water and Land Development*, 49, pp. 179–187. Available at: <https://doi.org/10.24425/jwld.2021.137110>.

Elman, J.L. (1990) "Finding structure in time," *Cognitive Science*, 14(2), pp. 179–211. Available at: [https://doi.org/10.1207/s15516709cog1402\\_1](https://doi.org/10.1207/s15516709cog1402_1).

En-nkhili, H. et al. (2020) "Application of water quality index for the assessment of Boudaroua Lake in the Moroccan Pre-Rif," *Proceedings of the 4th Edition of International Conference on Geo-IT and Water Resources 2020, Geo-IT and Water Resources 2020*, 36, pp. 1–5. Available at: <https://doi.org/10.1145/3399205.3399248>.



- En-nkhili, H. *et al.* (2021) "Water hydrochemistry of Lake Boudaroua in the Moroccan Prerifwest Mediterranean region," *E3S Web of Conferences*, 234, 00078.
- En-nkhili, H., Igouzal, M. and Etebaai, I. (2022) "Water quality assessment of an artificial small-scale reservoir in the Moroccan Pre-Rif: a case study of Boudaroua Lake using multivariate statistical techniques and self-organizing maps," *Desalination and Water Treatment*, 260, pp. 279–290. Available at: <https://doi.org/10.5004/dwt.2022.28533>.
- Etebaai, I., Damnati, B. and Taieb, M. (2010) "L'environnement du plan d'eau sidi Boudaroua : physico-chimie des eaux et sédimentation actuelle (Région d'Ouezzane, Maroc) [The environment of the water body sidi Boudaroua: Physico-chemistry of the water and current sedimentation (Ouezzane region, Morocco)]," *Geomaghreb*, 6, pp. 69–78.
- Gianniou, S.K. and Antonopoulos, V.Z. (2007) "Evaporation and energy budget in Lake Vegoritis, Greece," *Journal of Hydrology*, 345(3–4), pp. 212–223. Available at: <https://doi.org/10.1016/j.jhydrol.2007.08.007>.
- Hojjati, E. *et al.* (2021) "Estimating evaporation from reservoirs using energy budget and empirical methods: Alavian Dam reservoir, NW Iran," *Italian Journal of Agrometeorology*, 2, pp. 19–34. Available at: <https://doi.org/10.13128/IJAM-1033>.
- Hunt, A. *et al.* (2020) "Predicting water cycle characteristics from percolation theory and observational data," *International Journal of Environmental Research and Public Health*, 17(3), p. 734. Available at: <https://doi.org/10.3390/ijerph17030734>.
- Hussein, M.A.M. (2017) "Evaporation and evaluation of seven estimation methods: Results from Brullus Lake, north of Nile Delta, Egypt," *Hydrology*, 5(4), pp. 58–66. Available at: <https://doi.org/10.11648/j.hyd.20170504.12>.
- Igouzal, M. and Maslouhi, A. (2005) "Elaboration of management tool of a reservoir dam on the Sebou river (Morocco) using an implicit hydraulic model," *Journal of Hydraulic Research*, 43(2), pp. 125–130. Available at: <https://doi.org/10.1080/00221686.2005.9641228>.
- Jhajharia, D. *et al.* (2009) "Temporal characteristics of pan evaporation trends under the humid conditions of northeast India," *Agricultural and Forest Meteorology*, 149(5), pp. 763–770. Available at: <https://doi.org/10.1016/j.agrformet.2008.10.024>.
- Karami, H. *et al.* (2021) "Investigating the performance of neural network based group method of data handling to pan's daily evaporation estimation (Case study: Garmsar City)," *Journal of Soft Computing in Civil Engineering*, 5, pp. 1–18. Available at: <https://doi.org/10.22115/SCCE.2021.274484.1282>.
- Kisi, O. (2015) "Pan evaporation modeling using least square support vector machine, multivariate adaptive regression splines and M5 model tree," *Journal of Hydrology*, 528, pp. 312–320. Available at: <https://doi.org/10.1016/j.jhydrol.2015.06.052>.
- Majidi, M. *et al.* (2015) "Estimating evaporation from lakes and reservoirs under limited data condition in a semi-arid region," *Water Resources Management*, 29(10), pp. 3711–3733. Available at: <https://doi.org/10.1007/s11269-015-1025-8>.
- Malik, A., Kumar, A. and Kisi, O. (2017) "Monthly pan-evaporation estimation in Indian central Himalayas using different heuristic approaches and climate based models," *Computers and Electronics in Agriculture*, 143, pp. 302–313. Available at: <https://doi.org/10.1016/j.compag.2017.11.008>.
- Malik, A., Kumar, A. and Rai, P. (2018) "Weekly pan-evaporation simulation using MLP, CANFIS, MLR and climate-based models at Pantnagar," *Indian Journal of Ecology*, 45(2), pp. 292–298.
- National Centers for Environmental Prediction/National Weather Service/NOAA/U.S. Department of Commerce (2015) *NCEP GDAS/FNL 0.25 degree global tropospheric analyses and forecast grids*. Research Data Archive at the National Center for Atmospheric Research, Computational and Information Systems Laboratory. Available at: <https://doi.org/10.5065/D65Q4T4Z>. [Updated daily].
- Patle, G.T., Chettri, M. and Jhajharia, D. (2020) "Monthly pan evaporation modelling using multiple linear regression and artificial neural network techniques," *Water Science & Technology: Water Supply*, 20(3), pp. 800–808. Available at: <https://doi.org/10.2166/ws.2019.189>.
- Rosenberry, D.O. *et al.* (2007) "Comparison of 15 evaporation methods applied to a small mountain lake in the northeastern USA," *Journal of Hydrology*, 340(3–4), pp. 149–166. Available at: <https://doi.org/10.1016/j.jhydrol.2007.03.018>.
- Shafaei, M. *et al.* (2016) "A wavelet-SARIMA-ANN hybrid model for precipitation forecasting," *Journal of Water and Land Development*, 28, pp. 27–36. Available at: <https://doi.org/10.1515/jwld-2016-0003>.
- Sturrock, A.M., Winter, T.C. and Rosenberry, D.O. (1992) "Energy budget evaporation from Williams Lake: A closed lake in north central Minnesota," *Water Resources Research*, 28 (6), pp. 1605–1617. Available at: <https://doi.org/10.1029/92WR00553>.
- Tayfur, G. and Singh, V.P.R. (2005) "Predicting longitudinal dispersion coefficient in natural streams by artificial neural network," *Journal of Hydraulic Engineering*, 131, pp. 991–1000. Available at: [https://doi.org/10.1061/\(ASCE\)0733-9429\(2005\)131:11\(991\)](https://doi.org/10.1061/(ASCE)0733-9429(2005)131:11(991)).
- Wang, B. *et al.* (2019) "Evaluation of ten methods for estimating evaporation in a small high-elevation lake on the Tibetan Plateau," *Theoretical and Applied Climatology*, 136(3–4), pp. 1033–1045. Available at: <https://doi.org/10.1007/s00704-018-2539-9>.
- Wang, L. *et al.* (2017) "Pan evaporation modeling using six different heuristic computing methods in different climates of China," *Journal of Hydrology*, 544, pp. 407–427. Available at: <https://doi.org/10.1016/j.jhydrol.2016.11.059>.
- Winter, T.C. *et al.* (2003) "Evaporation determined by the energy-budget method for Mirror Lake, New Hampshire," *Limnology and Oceanography*, 48(3), pp. 995–1009. Available at: <https://doi.org/10.4319/lo.2003.48.3.0995>.